Supplementary Figure 1

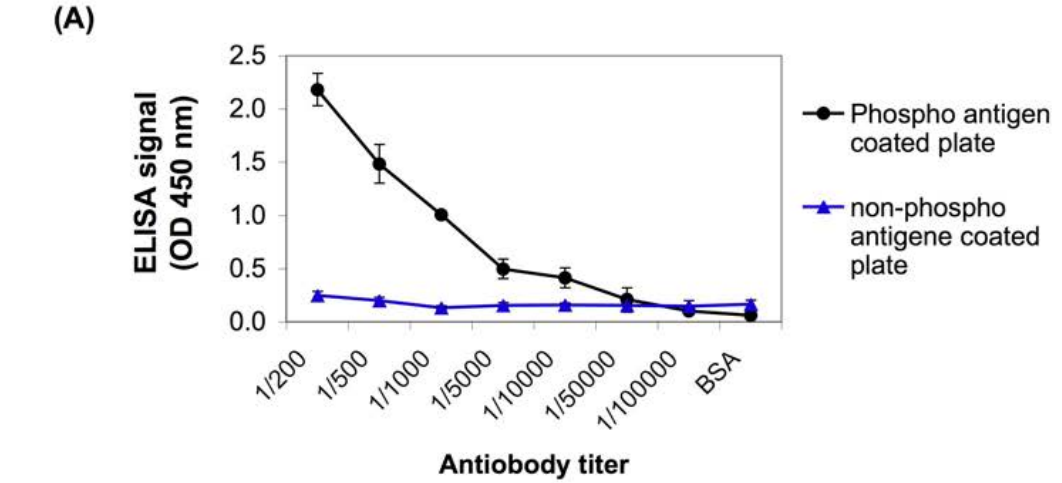

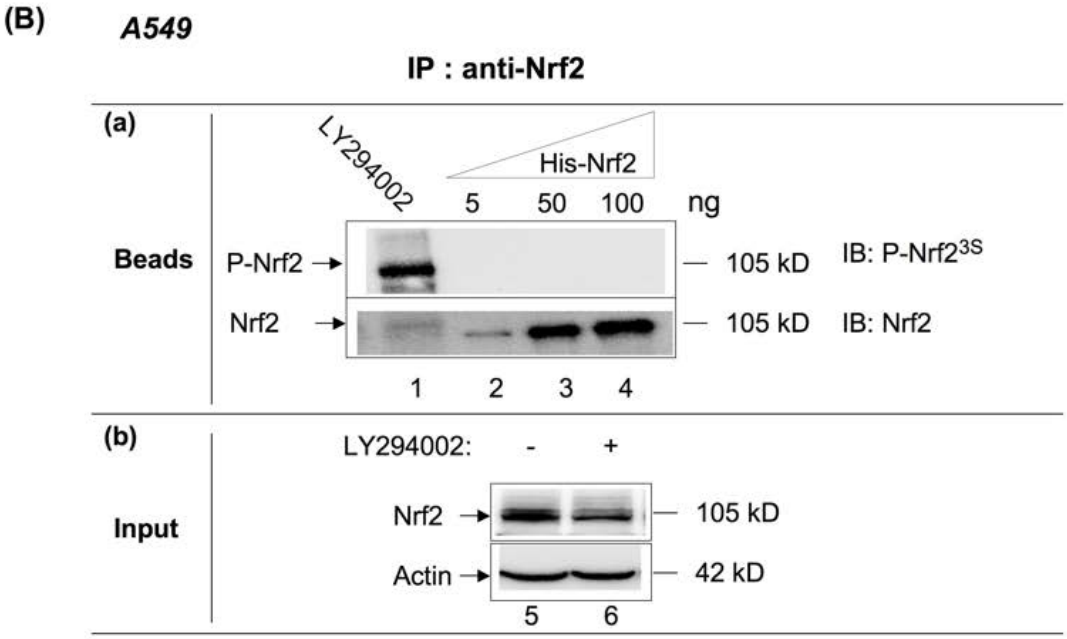

Supplementary Figure 2

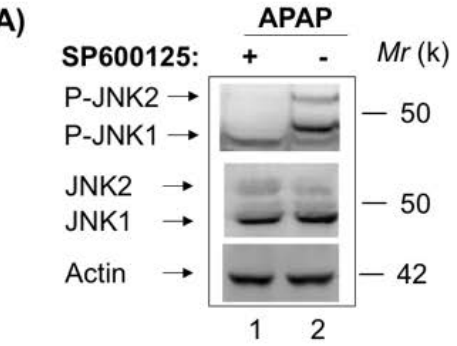

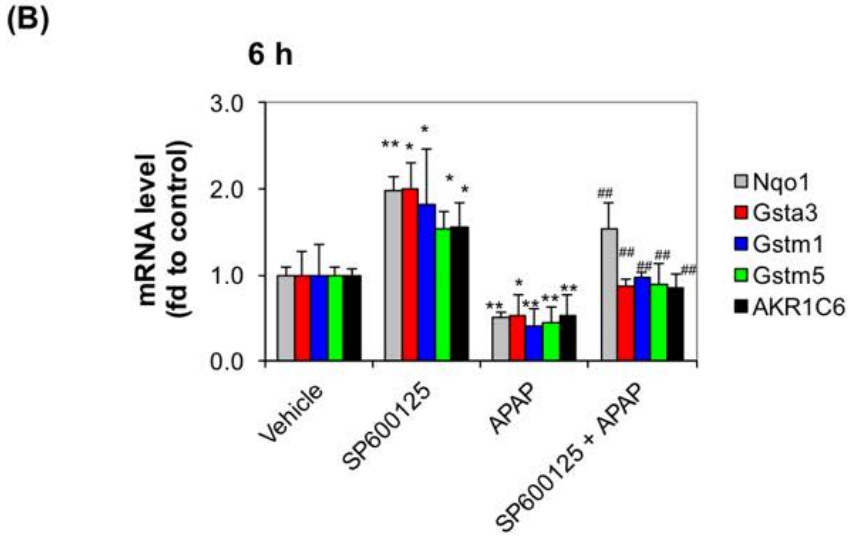

Supplementary Figure 3

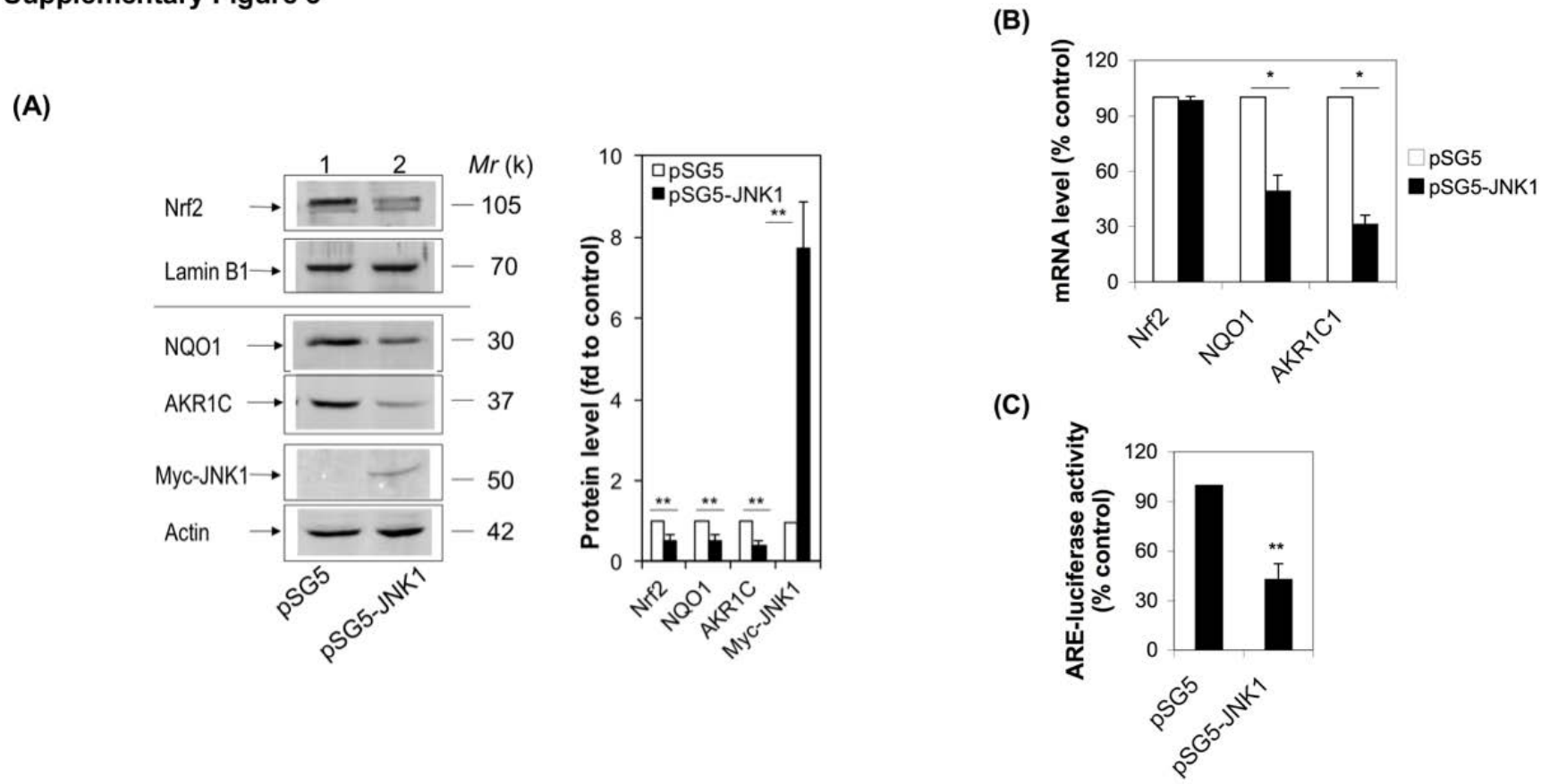

Supplementary Figure 4

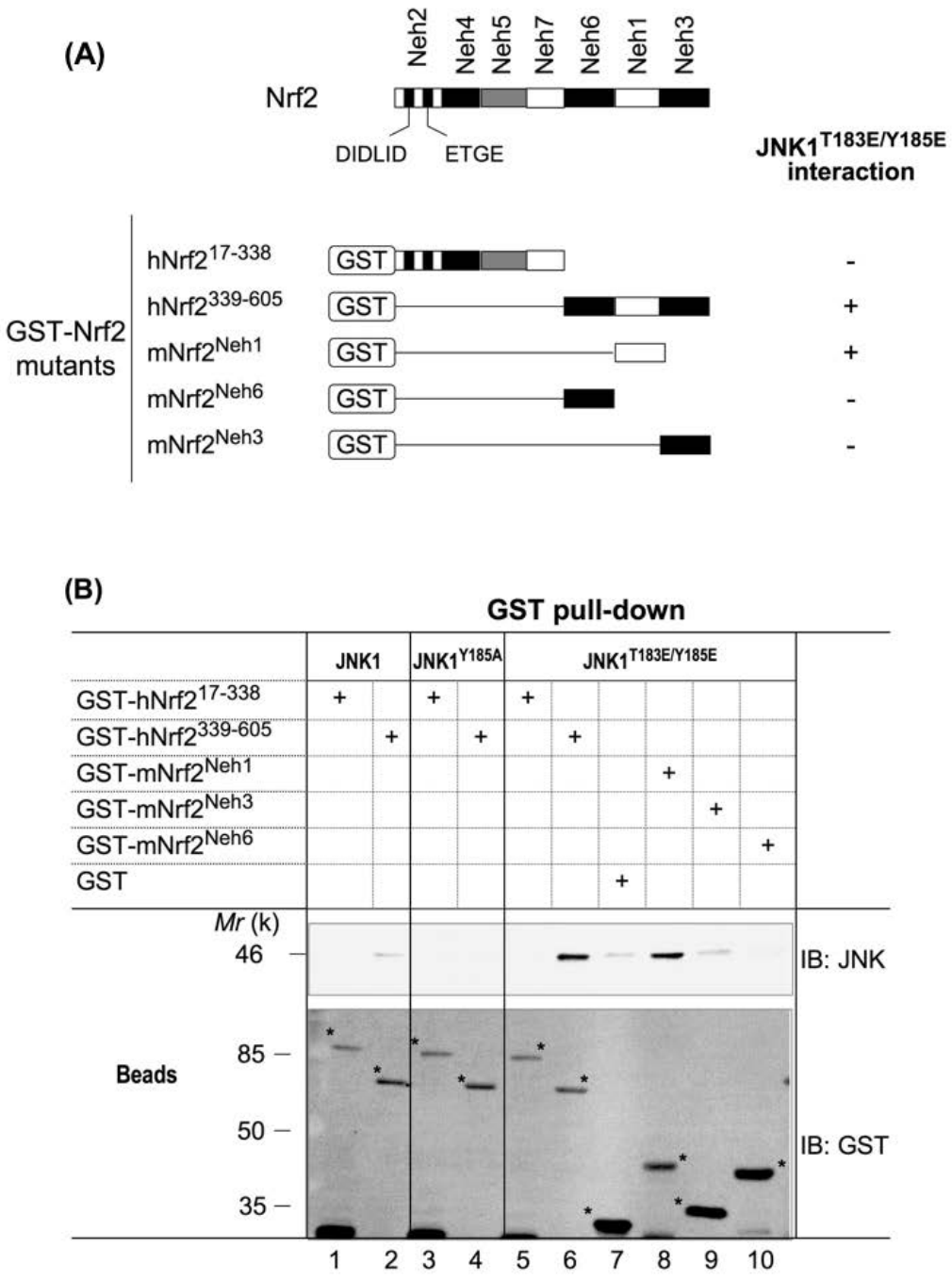

Supplementary Figure 5

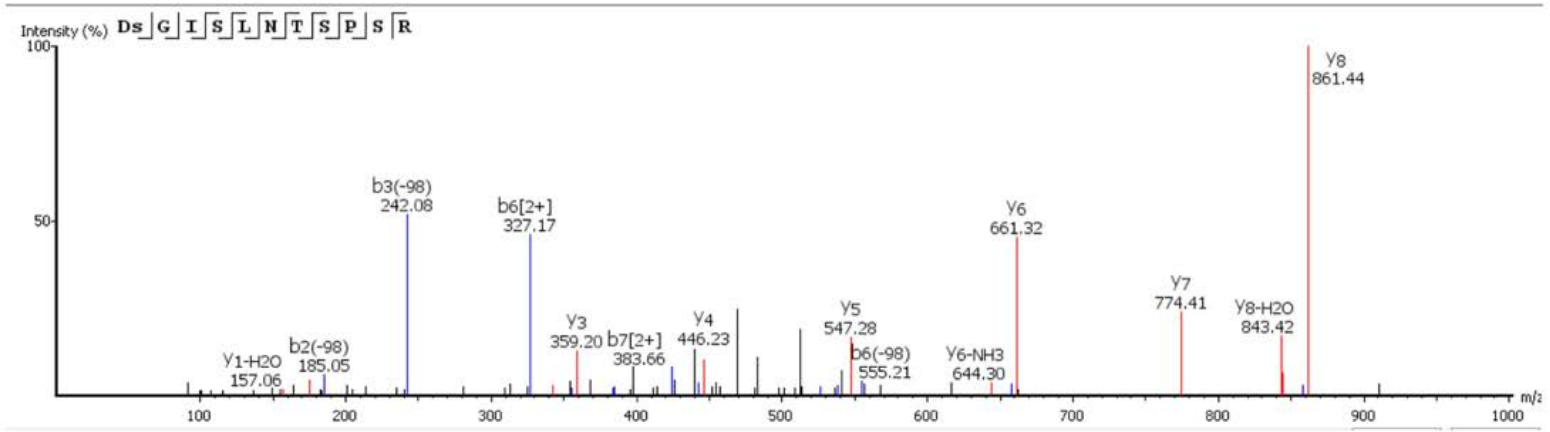

Supplementary Figure 6

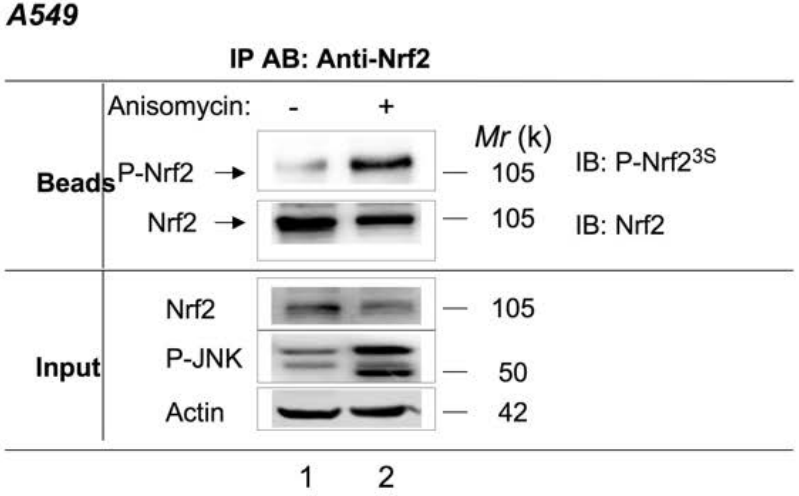

Supplementary Figure 7

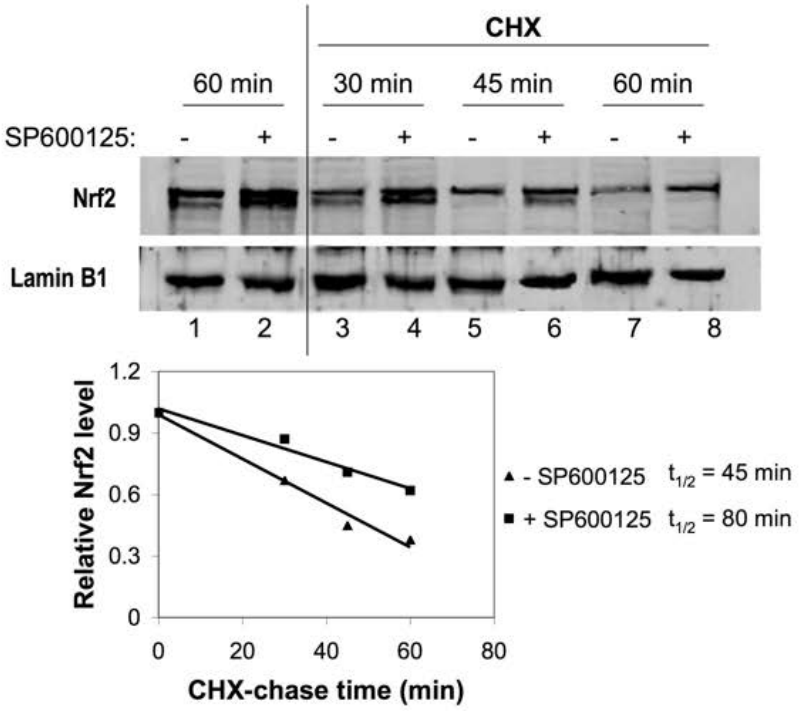

Supplementary Figure 8

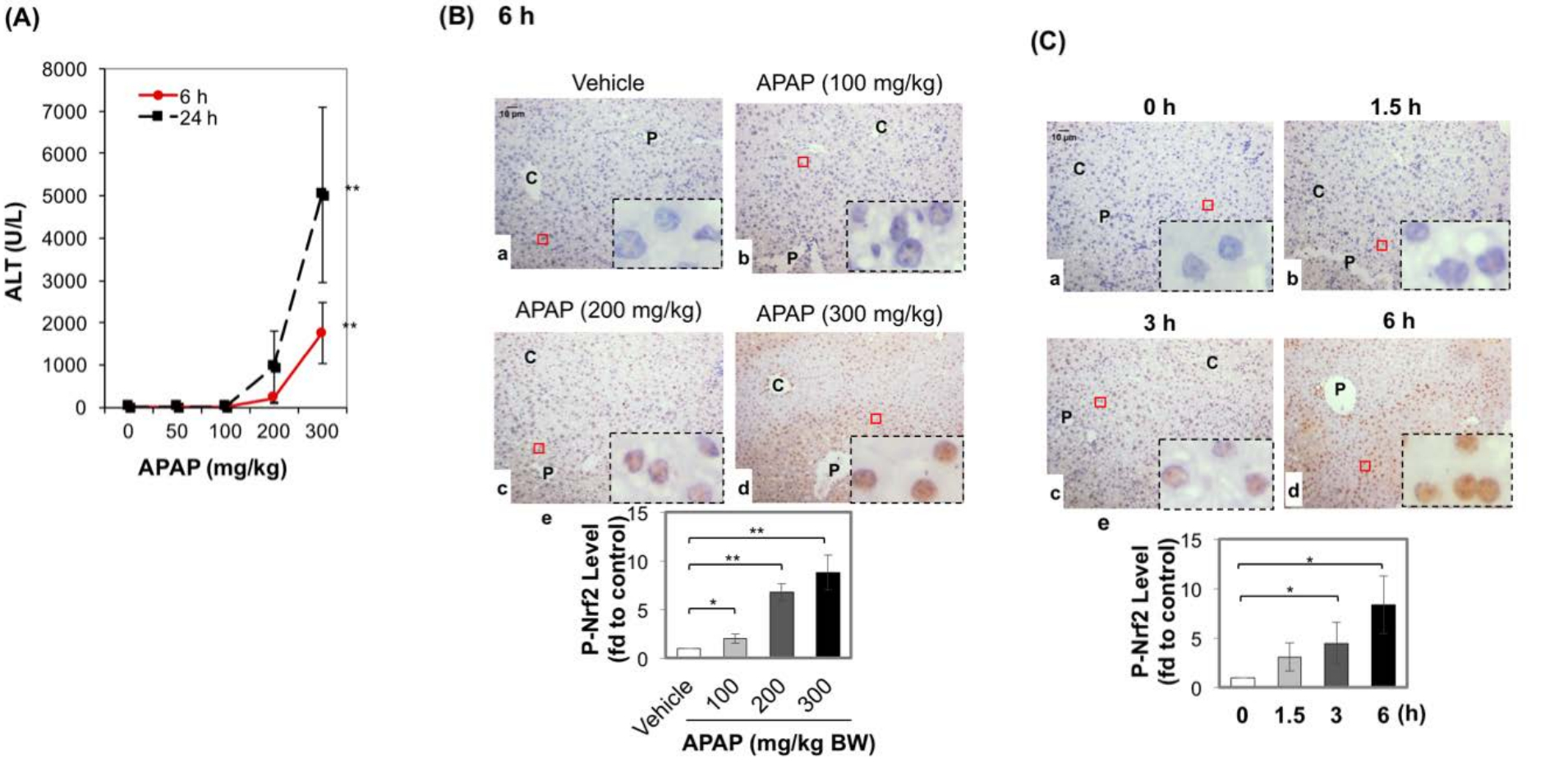

Supplementary Figure 9

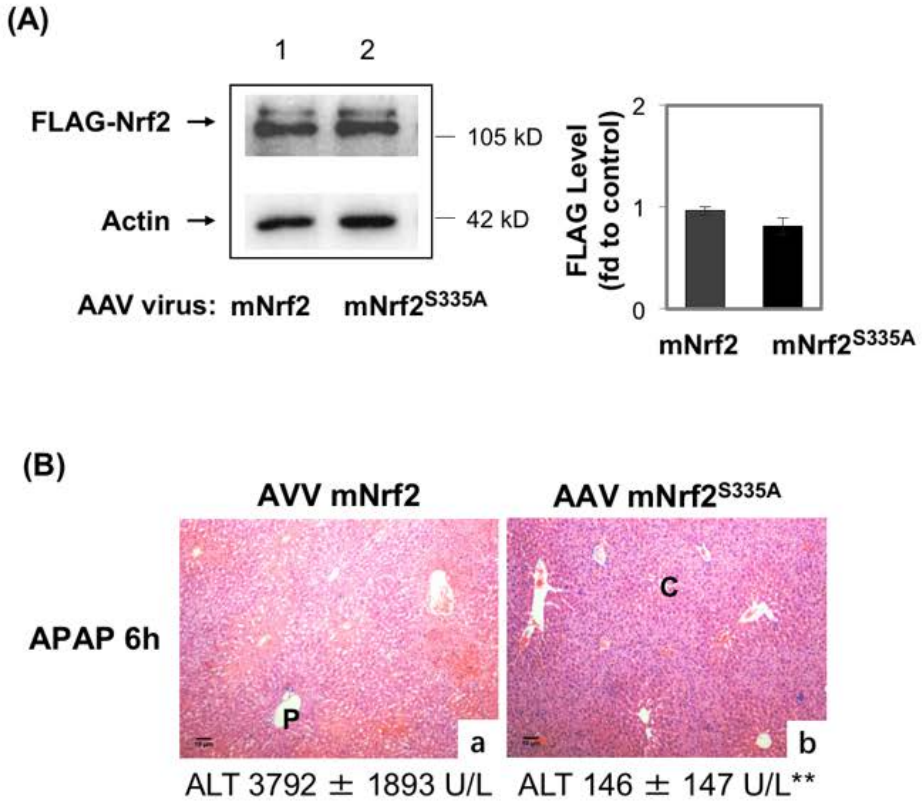

Supplementary Figure 10

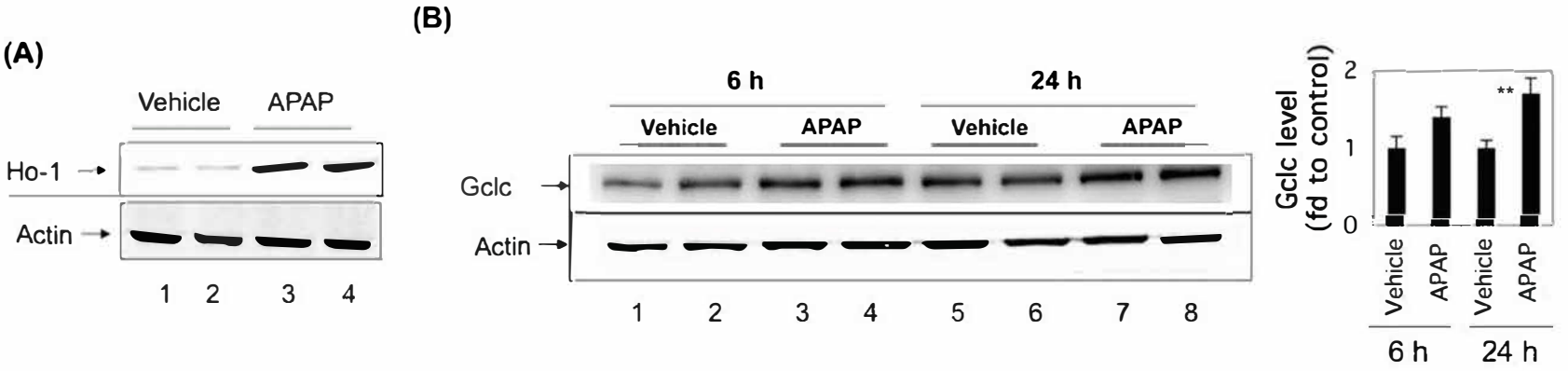

Supplementary Figure 11

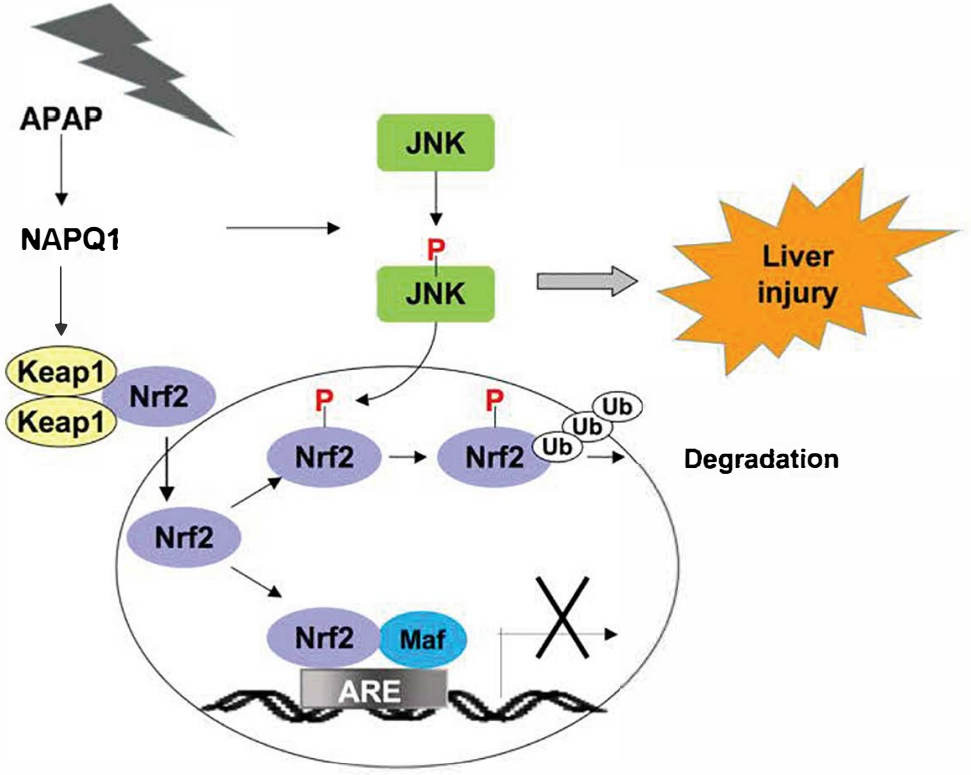

SUPPLEMENTARY INFORMATION

MATERIALS AND METHODS

Chemicals

Unless otherwise stated, all chemicals were from Sigma-Aldrich Co., Ltd (Shanghai, China). Antibody against mouse Nrf2 (H300; sc-13032) was from Santa Cruz Biotechnology (Shanghai, China). Antiserum against aldo-keto reductases 1C (AKR1C), Gst (glutathione S-transferase) α3, Gstm1, and Gstm5 were kindly provided by Prof. John Hayes (University of Dundee, UK). Anti-JNK1 antibodies (#ab129377 and #ab27709) were from Abcam (Shanghai, China). Anti-P-JNK (#9251) antibody was from Cell Signaling Technology (Danvers, MA, USA). Antibodies against NQO1 and HO-1 were raised in our laboratory as described previously (1).

Cell cultures

Keap1$^{+/+}$ and Keap1$^{-/-}$ mouse embryonic fibroblasts (MEFs) were kindly provided by Prof. Masayuki Yamamoto (University of Tsukuba, Japan). Human embryonic kidney HEK293 and NSCLC (non-small cell lung cancer) A549 cell lines were from the American Type Culture Collection (Beijing, China).

Plasmids

Plasmids pcDNA3.1/V5-mNrf2 encoding mouse (m) Nrf2 (full-length), and pcDNA3.1B/V5/his-mNrf2$^{\Delta ETGE}$ encoding mutant mNrf2 (lacking the ETGE motif), were kindly provided by Dr. Mike McMahon (University of Dundee, UK). PETDuet-1-His-hNrf2 coding His-tagged WT human (h) Nrf2$^{17\text{-}605}$, pET41a-hNrf2$^{17\text{-}338}$ coding the GST-tagged N-terminus of hNrf2, and pET41a-hNrf2$^{339\text{-}605}$ plasmids coding the C-terminus of Nrf2, were as described previously (2). pET41a-mNrf2^{Neh1} expressing the region coding amino-acids 427-554, pET41a-mNrf2^{Neh6} expressing the region coding amino-acids 318-403, and pET41a-mNrf2^{Neh3} expressing the region coding amino-acids 555-597 corresponding to the GST-tagged Neh1, Neh6, and Neh3 domains of mNrf2, respectively, were constructed by

PCR amplification from pEGFP-mNrf2 and cloning in-frame into the BamHI and XhoI, or the SalI and XhoI sites of pET41a. PETDuet-1-His-mNrf2$^{\Delta ETGE}$ was constructed by PCR amplification from pEGFP-mNrf2$^{\Delta ETGE}$(2) and cloning in-frame into the SacI and SalI sites of PETDuet-1. pcDNA3.1B/V5/his-mNrf2$^{\Delta ETGE,S335A}$ (lacking the ETGE motif and with Ser-335 replaced by alanine) was made from pcDNA3.1B/V5/his-mNrf2$^{\Delta ETGE}$ using the site-directed mutagenesis kit (Stratagene, China). pEGFP-mNrf2$^{\Delta ETGE,S335A}$ was made by subcloning from pcDNA3.1B/V5/his-mNrf2$^{\Delta ETGE,S335A}$ via the KpnI and ApaI sites. PETDuet-1-His-mNrf2$^{\Delta ETGE,S335A}$ was then constructed by PCR amplification from pEGFP-mNrf2$^{\Delta ETGE,S335A}$ and cloning in-frame into the SacI and SalI sites of PETDuet-1. pcDNA3.1/V5-mNrf2^{S335A} encoding mNrf2 with Ser-335 replaced by alanine, was made from pcDNA3.1/V5-mNrf2 using the site-directed mutagenesis kit. pFuipw-mNrf2$^{\Delta ETGE}$ encoding the Flag-tagged mutant mNrf2 (lacking the ETGE motif) was made by PCR amplification using pEGFP-C1-mNrf2$^{\Delta ETGE}$ as the template, and cloning in-frame into the XbaI and ascI sites of the lentiviral transfer vector pFuipw, which was kindly provided by Prof. Qimin Sun (Zhejiang University School of Medicine, China). pEGFP-C1-mNrf2$^{\Delta ETGE\Delta SDS1}$ encoding EGFP-tagged mutant mNrf2 (lacking the ETGE motif and SDS1 region of amino-acids 329–341) was made from pEGFP-C1-mNrf2$^{\Delta ETGE}$ using the site-directed mutagenesis kit. pFuipw-mNrf2$^{\Delta ETGE\Delta SDS1}$ encoding Flag-tagged mutant mNrf2 (lacking the ETGE motif and SDS1 region) was made by PCR amplification using pEGFP-C1-mNrf2$^{\Delta ETGE\Delta SDS1}$ as the template, and cloning in-frame into the XbaI and ascI sites of the pFuipw vector. Full-length human JNK1 cDNA (RefSeq #: NM_139046.3) was amplified from the human cDNA library and cloned into the XhoI and BamHI sites of a modified pSG5 vector. pDSRed-JNK1 was then generated by PCR amplification using pSG5-JNK1 as the template, and cloning in-frame into the mammalian expression vector pDSRed-C1 (Clontech) via the XhoI and SalI restriction sites. pETDuet-1-JNK1 expressing His-tagged WT JNK1 were made by PCR amplification using pDSRed-JNK1 as the template, and cloning in-frame into the BamHI and SalI sites of the pETDuet-1 vector. pETDuet-1-JNK1^{Y185A}, encoding a mutant JNK with

Tyr^{185}replaced by alanine, was made from pETDuet-JNK1 using the site-directed mutagenesis kit. Similarly, pETDuet-1-JNK1$^{T183E/Y185E}$, encoding a mutant JNK in which Thr^{183} and Tyr^{185} were replaced by glutamic acid, was made from pETDuet-JNK1 using the site-directed mutagenesis kit. Plasmid AAV019-mNrf2 encoding Flag-mNrf2, was made by PCR amplification using pcDNA3.1B/V5/his-mNrf2 as the template, and cloning in-frame into the MluI and XhoI sites of the AAV virus expressing vector pHBAAV-TBG-MCS-P2A-zsgreen (Hanbio Biotechnology Co., Shanghai, China). Plasmid AAV019-mNrf2^{S335A} encoding Flag-mNrf2^{S335} was similarly made by subcloning from pcDNA3.1/V5-mNrf2^{S335A} into pHBAAV-TBG-MCS-P2A-zsgree. Sequences of cloning primers are provided in STable 1. All plasmids were verified by DNA sequencing.

Transfections and luciferase reporter gene activity

Lipofectamine 2000 (Invitrogen), was used for transfection of plasmids. Empty vectors were used as negative controls for transfection experiments with plasmids. The reporter plasmids pGL-GSTA2.41bp-ARE along with pRL-TK, which encodes Renilla luciferase as an internal control, were used for transient transfection. The dual luciferase activity was determined as described elsewhere (3).

Real-time quantitative PCR (RT-qPCR)

Total RNA was prepared using TRIzol reagent (Invitrogen) and reverse-transcribed using oligo-dT primer and SuperScript II reverse transcriptase (Invitrogen) as described previously (3). RT-qPCR using validated SYBR® Green or TaqMan assays were carried out on a LightCycler® 480 instrument (Roche, Germany). All primers and probes were synthesized by TaKaRa Biotechnology. The primers and probes for detecting human Nrf2, NQO1, and AKR1C1 were as described previously (3). The primers for detecting mouse Gclc, Ho-1, Nqo1, Gstα3, Gstm1, Gstm3 were provided elsewhere (4). The sequences of the primers for detecting mouse Gclm in SYBR® Green assays are 5’-CACAGGTAAAACCCAATAGTAACCAAGT-3’ (forward) and

5’-GTGAGTCAGTAGCTGTATGTCAAATTGTT-3’ (reverse). The sequences of the primers for detecting mouse AKR1C6 in SYBR® Green assays are 5’-AGCAGATGGCACTGTGAAGAGG-3’(forward) and 5’-CAGGTCCACATAGTCCAACTGG-3’ (reverse).

Chromatin immunoprecipitation (ChIP) assay

ChIP assays were performed as described previously (3). The sequences of the primers detecting the AREs in the promoter of NQO1 and GAPDH were described elsewhere (3). The sequences of the primers detecting the ARE in the AKR1C1 promoter were 5’-TTTACAACCTCCCCTGCTTG-3’ (forward) and 5’-TGAGACGTCTGCCTTGTCTG-3’ (reverse). The relative binding of Nrf2 to ARE sites was calculated by quantification of band intensity with the Odyssey infrared imaging system (LI-COR® Biosciences) normalized to that of the input.

GST pulldown, immunoprecipitation, and Western blot analysis

Mutant forms of Nrf2 fused to GST were expressed in *E. coli* cells and purified with glutathione-Sepharose beads (Pharmacia, China). The purified proteins were visualized by staining with Coomassie blue. The GST pull-down assay was carried out as described previously(2). Approximately 2 μg of purified GST-bound mutant proteins and His-tagged protein were used for the pull-down assay. The beads were washed five times before collection by centrifugation. The bound proteins were analyzed by SDS-PAGE, followed by immunoblotting with antibody against GST or the indicated protein. The immune complexes were analyzed by immunoblotting with an antibody directed against JNK or GST.

Preparation of protein samples, SDS-PAGE gels, and immunoblotting was as described previously (3, 5). Immunoblotting with antibody against actin was used to confirm equal loading of whole-cell extracts, while lamin B1 was used as loading control for nuclear extracts. The relative levels of the proteins of interest were calculated by quantification of band intensity with an Odyssey infrared imaging system (LI-COR® Biosciences) and

normalized to actin or lamin B1.

In vitro phosphorylation assay

Mutant forms of Nrf2 with fused His were expressed in *E. coli* cells and purified with Ni-NTA resins (ThermoFisher Scientific, Waltham, MA, USA) following the manufacturer's instructions. To detect Nrf2 phosphorylation by JNK, kinase assays were carried out as described previously (6). Briefly, HEK293 cells were treated with the JNK activator anisomycin (5 μg/ml) for 30 min (7), and then the cell lysate was subjected to immunoprecipitation with anti-P-JNK. The immunoprecipitates were washed in buffer containing 50 mM Hepes pH 7.2, 10 mM $MgCl_2$, 1 mM EGTA, and 0.01% Triton X-100. The samples were then incubated with appropriate purified His-Nrf2 WT or mutant proteins in the same buffer supplemented with ATP (100 μM) and dithiothreitol (2 mM). After incubation at 30°C for 30 min, the reaction was stopped by 5×SDS sample buffer. The phosphorylated Nrf2 products were analyzed by immunoblotting with anti-P-Nrf2^{3S}. The total Nrf2 products including the phosphorylated and the non-phosphorylated proteins were analyzed by immunoblotting with anti-Nrf2 (Santa Cruz, H300; sc-13032).

Mass spectrometric analysis

HEK293 cells were treated with 5 μg/ml anisomysin for 30 min. The cell lysate was subjected to immunoprecipitation with anti-P-JNK. The immunoprecipitates were subjected to *in vitro* kinase assays with purified recombinant His-mNrf2, followed by SDS-PAGE. The gel was stained with Coomassie Blue, and the band corresponding to Nrf2 was cut out of the gel and digested in-gel with trypsin followed by LC/MS/MS on an Obitrap-XL mass spectrometer (Thermo Fisher Scientific, Waltham, MA, USA). In-gel digestion and mass spectrometric analysis were performed at the National Center for Protein Science Shanghai (Shanghai, PR China). Proteins were identified by a search of the fragment spectra against the National SwissProt protein database (EBI) using Mascot v.2.3 (Matrix Science, London, UK) and Sequest (v.1.20) via Proteome Discoverer v.1.3 (Thermo Fisher Scientific). Phosphopeptide matches were analyzed using PhosphoRS implemented in Proteome

Discoverer and manually curated (8).

ELISA for antibody characterization

ELISA was carried out using a kit from Sigma (Shanghai, China) according to the manufacturer's instructions. Briefly, the wells of microtiter plates were coated by overnight incubation with 50 μl antigen peptide (10 μg/ml) in bicarbonate coating buffer at 4°C, and blocked by 2 h-incubation with 200 μl 0.1% BSA in TBST (Tris-buffered saline pH 7.4 with 0.05% Tween20) at room temperature followed by washing with TBST. The wells were then incubated with 100 μl primary rabbit antibody at dilutions of 1:200 and 1:100000 in TBST for 1 h at room temperature followed by washing. The wells were incubated with secondary goat anti-rabbit HRP-conjugated antibody. After washing, the substrate SIGMAFAST^{TM} OPD was added. After 30 min incubation, absorbance at 450 nm was recorded.

Preparation of lentiviral transduction particles and generation of the stable cell lines 293T-mNrf2$^{\Delta E}$ and 293T-mNrf2$^{\Delta E\Delta SDS1}$

psPAX2 andpMD2.G were kindly provided by Dr. Trono (9). HEK293T cells were transfected with the lentiviral transfer vector pFuipw-mNrf2$^{\Delta ETGE}$ or pFuipw-mNrf2$^{\Delta ETGE\Delta SDS1}$, together with psPAX2 packaging andpMD2.G envelope plasmid DNA using Lipofectamine^{TM} 2000 following the manufacturer's instructions (Invitrogen, Shanghai, China). The supernatants were harvested at 24 h, 36 h, and 48 h after transfection. The viral particles were purified using a 0.45-μm filter, and concentrated in PEG8000 as described previously (10). The purified viral particles were re-suspended in HBSS buffer and used to infect HEK293T cells followed by selection in 0.5 μ g/mL puromycin as described elsewhere (10). A single-colony cell line stably expressing Flag-mNrf2$^{\Delta ETGE}$ after many passages, defined as 293T-mNrf2$^{\Delta E}$, was generated and used for this study. Similarly, a single-colony cell line stably expressing Flag-mNrf2$^{\Delta ETGE\Delta SDS1}$, defined as 293T-mNrf2$^{\Delta E\Delta SDS1}$, was generated and used for this study.

Immunohistochemical analysis (IHC)

Hematoxylin/eosin staining and immunohistochemical analysis of sections from mouse livers were as described previously (1, 11). Immunoreactivity was quantified using IPP 6.0 image analysis software (Media Cybernetics, USA) as described previously (12-14). The results of IHC were based on the average value from three mice per group. In each mouse, three separate slides were analyzed. Images were captured under a light microscope (Olympus BX41, Shanghai, China) at 100×, 200×, 400× or 1000× magnification. Image Pro Plus 6.0 software (Media Cybernetics, Inc.) was used to analyze the staining intensity. Five microscopic fields in tissues at 100× magnification were randomly selected, the integral optical density (IOD) was calculated, and this was considered to be the expression level. Higher IOD values represented greater antigen expression. For P-Nrf2, nuclear staining density was analyzed (15, 16). The percentage of necrotic area was analyzed semi-quantitatively as described previously(17), using image analysis with ImageJ software following the user's guide (http://imagej.net/docs/guide).

Cycloheximide (CHX) chase assay

A549 cells were treated with 20 μM CHX for various time intervals and then lysed in 2× SDS sample buffer. The samples were analyzed by Western blot with anti-Nrf2 antibodies.

Primary hepatocyte culture and exposure to APAP

Mouse liver was perfused with 0.05% Collagenase Type IV (Sigma-Aldrich, China) as described previously(18). The viability of the isolated hepatocytes was 90% as judged by trypan blue exclusion. Isolated hepatocytes were suspended in William E medium containing 5% foetal calf serum, 10^{-6}M insulin, 10^{-4}M hydrocortisone-21-hemisuccinate, 60 μg/ml gentamicin. 1.2×10^6 cells in 4 ml were plated in individual 60-mm culture dishes coated with 0.03% collagen (Sigma) and cultured in a 5% CO2 atmosphere at 37 °C. After 3 h, the culture medium was changed with serum-free medium containing 10 mM APAP. After 0.5–2 h culture, hepatocytes were harvested. DMSO (0.1% v/v) was used as vehicle. Levels of P-JNK and P-Nrf2 were analyzed by immunoblotting.

Knockdown of JNK using small interfering RNA–expressing adenoviruses

Small interfering RNA (siRNA) sequences for targeting mouse JNK1 (5′-GCAGAAGCAAACGTGACAACA-3′ and 5′-GCAGAAGCAAACGTGACAACA-3′), JNK2 (5′-CTCAACTTTCACTGTTCTAAA-3′ and 5′-CCGCAGAGTTCATGAAGAA-3′), and control (5′-CCTTCCCTGAAGGTTCCTCC-3′) were designed by Sigma-Aldrich (Shanghai, China). The oligoes were individually cloned into the pAdTrace-61 vector (from Dr. Qimin Sun, Zhejiang University, China). After recombination with pAdEasy-1 vector in BJ5183-AD-1 electrocompetent cells (Agilent Technologies, Santa Clara, CA), an equal amount of each individual plasmid for knocking down both JNK1 and JNK2 (JNK), were pooled together. High-titer viruses (~10^{11} plaque-forming units) were generated in 293 cells as described (19). To achieve knockdown of JNK in mouse livers, 2-month-old male C57BL/6J mice were injected intravenously by tail vein with adenoviruses expressing JNK, or control siRNA (5×10^9 PFU per mouse) for 10 days. Mice were then treated with either APAP (300 mg/kg i.p.) or PBS (i.p.) for 6 h and 24 h, followed by blood and liver collection, ALT and Western blotting analysis.

in vivo expressing WT or mutant mNrf2 in *Nrf2*$^{-/-}$ mice using AAV virus

AAV-293 cells were transfected with AAV019-mNrf2 or AAV019-mNrf2^{S335A}, together with pAAV-RC and pHelper using Lipofectamine™ 2000 following the manufacturer's instructions (Invitrogen). The supernatants were harvested at 72 h after transfection. HBAAV2/9-GFP (Hanbio Biotechnology Co., Shanghai, China) was used as control AAV virus. The viral particles were purified using Biomiga AAV Purification Maxi Kit (Biomiga, Inc., San Diego, California, USA) by following the manufacturer's instructions. To express mNrf2 or mNrf2^{S335A} in *Nrf2*$^{-/-}$ mouse livers, 2-month-old male C57BL/6J *Nrf2*$^{-/-}$ mice were injected intravenously by tail vein with AAV viurs expressing mNrf2, mNrf2^{S335A} or control AAV virus (1×10^{11} PFU per mouse) for 21 days. Mice were then treated with either APAP

(300 mg/kg i.p.) or PBS (i.p.) for 6 h, followed by blood and liver collection, ALT and Western blotting analysis.

REFERENCES

1. Luo L, Chen Y, Wu D, Shou J, Wang S, Ye J, Tang X, et al. Butylated hydroxyanisole induces distinct expression patterns of Nrf2 and detoxification enzymes in the liver and small intestine of C57BL/6 mice. Toxicol Appl Pharmacol 2015;288:339-348.

2. Wang H, Liu K, Geng M, Gao P, Wu X, Hai Y, Li Y, et al. RXRalpha Inhibits the NRF2-ARE Signalling Pathway Through A Direct Interaction With the Neh7 domain of NRF2. Cancer Res 2013;73:3097-3108.

3. Tang X, Wang H, Fan L, Wu X, Xin A, Wang XJ. Luteolin inhibits NRF2 leading to negative regulation of the NRF2/ARE pathway and sensitization of human lung carcinoma A549 cells to therapeutic drugs. Free Radic Biol Med 2011;50:1599-1609.

4. Luo L, Chen Y, Wang H, Wang S, Liu K, Li X, Wang XJ, et al. Mkp-1 protects mice against toxin-induced liver damage by promoting the Nrf2 cytoprotective response. Free Radic Biol Med 2017;115:361-370.

5. Chian S, Li YY, Wang XJ, Tang XW. Luteolin sensitizes two oxaliplatin-resistant colorectal cancer cell lines to chemotherapeutic drugs via inhibition of the Nrf2 pathway. Asian Pac J Cancer Prev 2014;15:2911-2916.

6. Huntwork-Rodriguez S, Wang B, Watkins T, Ghosh AS, Pozniak CD, Bustos D, Newton K, et al. JNK-mediated phosphorylation of DLK suppresses its ubiquitination to promote neuronal apoptosis. J Cell Biol 2013;202:747-763.

7. Lee TL, Shyu YC, Hsu PH, Chang CW, Wen SC, Hsiao WY, Tsai MD, et al. JNK-mediated turnover and stabilization of the transcription factor p45/NF-E2 during differentiation of murine erythroleukemia cells. Proc Natl Acad Sci U S A 2009;107:52-57.

8. Taus T, Kocher T, Pichler P, Paschke C, Schmidt A, Henrich C, Mechtler K. Universal and confident phosphorylation site localization using phosphoRS. J Proteome Res 2011;10:5354-5362.

9. Dull T, Zufferey R, Kelly M, Mandel RJ, Nguyen M, Trono D, Naldini L. A third-generation lentivirus vector with a conditional packaging system. J Virol 1998;72:8463-8471.

10. Cheng X, Ma X, Ding X, Li L, Jiang X, Shen Z, Chen S, et al. Pacer Mediates the Function of Class III PI3K and HOPS Complexes in Autophagosome Maturation by Engaging Stx17. Mol Cell 2017;65:1029-1043 e1025.

11. Luo L, Chen Y, Wu D, Shou J, Wang S, Ye J, Tang X, et al. Differential expression patterns of Nqo1, AKR1B8 and Ho-1 in the liver and small intestine of C57BL/6 mice treated with sulforaphane. Data Brief 2015;5:416–423.

12. Shi H, Hayes M, Kirana C, Miller R, Keating J, Macartney-Coxson D, Stubbs R. TUFM is a potential new prognostic indicator for colorectal carcinoma. Pathology 2012;44:506-512.

13. Li J, Qu Y, Chen D, Zhang L, Zhao F, Luo L, Pan L, et al. The neuroprotective role and mechanisms of TERT in neurons with oxygen-glucose deprivation. Neuroscience 2013;252:346-358.

14. Wang CJ, Zhou ZG, Holmqvist A, Zhang H, Li Y, Adell G, Sun XF. Survivin expression quantified by Image Pro-Plus compared with visual assessment. Appl Immunohistochem Mol Morphol 2009;17:530-535.

15. Mady HH, Melhem MF. FHIT protein expression and its relation to apoptosis, tumor histologic grade and prognosis in colorectal adenocarcinoma: an immunohistochemical and image analysis study. Clin Exp Metastasis 2002;19:351-358.

16. Francisco JS, Moraes HP, Dias EP. Evaluation of the Image-Pro Plus 4.5 software for automatic counting of labeled nuclei by PCNA immunohistochemistry. Braz Oral Res 2004;18:100-104.

17. Valledor AF, Xaus J, Comalada M, Soler C, Celada A. Protein kinase C epsilon is required for the induction of mitogen-activated protein kinase phosphatase-1 in lipopolysaccharide-stimulated macrophages. J Immunol 2000;164:29-37.

18. Wang XJ, Hodgkinson CP, Wright MC, Paine AJ. Temperature-sensitive mRNA degradation is an early event in hepatocyte de-differentiation. Biochem J 1997;328 (Pt

3):937-944.

19. Luo J, Deng ZL, Luo X, Tang N, Song WX, Chen J, Sharff KA, et al. A protocol for rapid generation of recombinant adenoviruses using the AdEasy system. Nat Protoc 2007;2:1236-1247.

20. Chowdhry S, Zhang Y, McMahon M, Sutherland C, Cuadrado A, Hayes JD. Nrf2 is controlled by two distinct beta-TrCP recognition motifs in its Neh6 domain, one of which can be modulated by GSK-3 activity. Oncogene 2013;32:3765-3781.

21. Rada P, Rojo AI, Chowdhry S, McMahon M, Hayes JD, Cuadrado A. SCF/{beta}-TrCP promotes glycogen synthase kinase 3-dependent degradation of the Nrf2 transcription factor in a Keap1-independent manner. Mol Cell Biol 2011;31:1121-1133.

22. Rada P, Rojo AI, Evrard-Todeschi N, Innamorato NG, Cotte A, Jaworski T, Tobon-Velasco JC, et al. Structural and functional characterization of Nrf2 degradation by the glycogen synthase kinase 3/beta-TrCP axis. Mol Cell Biol 2012;32:3486-3499.

Supplementary figure legends

Supplementary Figure 1. Preparation and characterization of anti-P-Nrf2^{3S}. A keyhole-limpet hemocyanin-conjugated synthetic peptide corresponding to the phosphorylated SDS1 region of mouse Neh6 (20-22) was injected into rabbits to raise anti-phospho-Nrf2(335,338,342) antiserum. After the tenth booster injection, the anti- polyclonal antibody, defined as P-Nrf2^{3S}, was purified on an antigen peptide-coupled affinity column, followed by passage over a non-phosphorylated antigen peptide-coupled affinity column to remove antibodies against non-phosphorylated Nrf2. (A) ELISA characterization of anti-P-Nrf2^{3S}. ELISA was carried out as described in Supplementary Materials and Methods. The phospho-antigen peptide CEFNDSDpSGIpSLNTpSS or the non-phospho-peptide of CEFNDSDSGISLNTSS was used for coating. The primary antibody was anti-P-Nrf2^{3S}. BSA was used as negative control. The data shown represent results from four independent experiments. (B) Anti-P-Nrf2^{3S} recognizes the Ser cluster in the Neh6 domain of Nrf2 phosphorylated by GSK3β. It has been reported that LY294002, a PI3 kinase inhibitor, stimulates the phosphorylation of a Ser cluster in the Neh6 domain of Nrf2 via activating GSK3β (20-22). To induce phosphorylation at the Ser cluster in the Neh6 domain of Nrf2, A549 cells were serum-starved for 16 h before treatment with LY294002 (40 μM) for 2 h to activate GSK3β. The cell lysate was then subjected to immunoprecipitation with anti-Nrf2. The immunoprecipitate was probed with anti-Nrf2 or anti-P-Nrf2^{3S} (a, lane 1). (b) The input represents 5% of the total amount of lysate used for immunoprecipitation probed with anti-Nrf2. LY294002 reduced the abundance of Nrf2 (b, lane 6). (a, lanes 2-4) 5–100 ng of recombinant His-hNrf2. Anti-P-Nrf2^{3S} only reacted with the phosphorylated Nrf2 (a, lane 1), but not the non-phosphorylated Nrf2 (a, lanes 2-4), demonstrating the specificity of the antibody. IB, immunoblot.

Supplementary Figure 2. SP600125 inhibits the phosphorylation of JNK in APAP-treated liver. SP600125 (10 mg/kg i.p.) was given to WT mice 1 h prior to the injection of APAP (300 mg/kg i.p.). Livers were harvested 6 h after administration of APAP. (A) Western

immunoblots of protein extracts from livers were probed with anti-P-JNK1/2, anti-JNK1/2, or anti-actin. Blots represent results from at least three independent experiments. Each lane contains a sample from a single mouse. (B) mRNA levels of Nqo1, Gstα3, Gstm1, Gstm5, and AKR1C6 were analyzed by RT-qPCR. Value of the same mRNA from WT mice treated with vehicle was set at 1; 18S rRNA was used as internal control (mean±SD; n = 3; *p<0.05, ##p <0.01).

Supplementary Figure 3. Overexpression of JNK1 suppresses the expression of Nrf2 and the ARE gene battery. A549 cells were transfected with pSG5 or pSG5-JNK1. The nuclear extracts were probed with anti-Nrf2 and anti-lamin B1. Whole-cell lysates were probed by immunoblotting with anti-NQO1, anti-AKR1C, anti-HA, and anti-actin (A). The relative levels of indicated proteins normalized to lamin B1 or actin are shown in Right panel (A). The value for pSG5 treatment was set at 1. Values are mean ± SD. (n = 3). (B) Nrf2, AKR1C1, and NQO1 mRNA levels as determined by RT-PCR. 18S rRNA was used as internal control. The value for pSG5 was set at 100%. (C) Luciferase activity 24 h after transfection of A549 cells with pSG5 or pSG5-JNK1 plus pGL-GSTA2.41bp-ARE reporter vector and pRL. The value for pSG5 was set at 100%. Data are presented as the mean ± SD of triplicate experiments. *p <0.05, **p <0.01.

Supplementary Figure 4. P-JNK interacts with Neh1 in Nrf2. (A) Schematic of GST-tagged hNrf2 and mNrf2 mutants and their interactions with $JNK1^{T183E\text{-}Y185E}$. The regions of interest within Nrf2 are indicated by bars, and the amino-acid residues involved are indicated by the polypeptide designations. (B) GST-pulldown of His-JNK1, His-$JNK1^{Y185A}$, and His-$JNK1^{T183E/Y185E}$ with GST-tagged mutant Nrf2 proteins. The same amounts of GST protein or GST-Nrf2 mutant fusion protein, shown in (A), were incubated with purified recombinant His-JNK1, His-$JNK1^{Y185A}$, or His-$JNK1^{T183E/Y185E}$. The proteins bound to GSH-Sepharose were eluted, separated on SDS-PAGE and subjected to immunoblotting using

antibody against either JNK or GST (Beads, immunoprecipitates after the washing procedure; IB, immunoblot). Blots represent results from at least three independent experiments.

Supplementary Figure 5. mNrf2 peptide sequence data. HEK293 cells were treated with 5 μg/ml anisomysin for 30 min. The cell lysate was subjected to immunoprecipitation with anti-P-JNK. The immunoprecipitates were subjected to *in vitro* kinase assays with purified recombinant His-mNrf2, followed by SDS-PAGE. The gel was stained with Coomassie Blue, and the band corresponding to Nrf2 was cut out and digested in-gel with trypsin followed by LC/MS/MS. Mass spectrometric analysis of a tryptic fragment at m/z 182.054 (mass error, 0.10 p.p.m.) matched to the doubly-charged peptide DsGISLNTSPSR, suggesting that Ser-335 was phosphorylated. The Sequest score for this match was Xcorr = 4.4; Mascot scores were 27, and the expectation value was 5.1×10^{-4}. The best score evidence ID was 460, and the site probability was 98.47%.

Supplementary Figure 6. Activated JNK increases the phosphorylation of Nrf2 in A549 cells. A549 cells were treated with 5 μ g/mL anisomysin for 1 h. Whole-cell lysates were subjected to immunoprecipitation with anti-Nrf2. The immunoprecipitates were analyzed by immunoblotting using anti-Nrf2 or anti-P-Nrf2^{3S}. Input, 10% of the cell lysate used for immunoprecipitation. The results presented are typical examples from at least three independent experiments.

Supplementary Figure 7. SP600125 stabilizes Nrf2 in A549 cells. A549 cells were treated with 10 μM SP600125. CHX (20 μM) was added into each dish of cells to a final concentration of 20 μ M. Nuclear extracts were prepared after the indicated chase periods, and probed by immunoblotting with anti-Nrf2. The relative levels of Nrf2 were normalized to Lamin B1. The graph depicts the natural logarithm of the relative expression of Nrf2 as a

function of CHX chase time. The half-life derived from the slope of the best-fit line is indicated. Results are representative of three separate experiments.

Supplementary Figure 8. Nrf2 phosphorylation is dose- and time-dependent in APAP-induced liver injury. (A)-(B) WT mice were given 50 mg/kg, 100 mg/kg, 200 mg/kg or 300 mg/kg BW APAP (i.p.). Blood and livers were collected 6 h and 24 h later. (A) Serum ALT levels at 6 h and 24 h (n = 12–15). One-way ANOVA with post hoc Dunnett's test was used to test dose response effect by comparing groups to the control (Vehicle). **p <0.01. (B) Sections of livers from 3 randomly selected mice in Vehicle (a), 100 mg/kg (b), 200 mg/kg (c) or 300 mg/kg (d) APAP group at 6 h post APAP, were probed with anti-p-Nrf2^{3S}. (C) WT mice were given APAP (300 mg/kg BW i.p.). Livers were harvested 1.5 h, 3 h or 6 h later. Sections of livers in 3 randomly selected mice from each group were analyzed by IHC with anti-p-Nrf2^{3S}. (B)-(C) original magnification ×100; scale bars, 10 μm; insets, original magnification ×400; P, portal venules; C, central venules). (e) Statistics from experiments as in (a–d). The control (Vehicle) was set at 1. Values are mean ± SD (n = 3). *p <0.05, **p <0.01.

Supplementary Figure 9. Overexpression of mNrf2 and mNrf2^{S335A} in *Nrf2*$^{-/-}$ mice and APAP treatment. *Nrf2*$^{-/-}$ mice were treated with AAV019-mNrf2 or AAV019-mNrf2^{S335A} (1×10^{11} PFU per mouse i.v.) for 21 days, and then treated by APAP (300 mg/kg i.p.) or PBS for 6 h. (A) Western blotting of Flag-Nrf2 in 3 randomly selected *Nrf2*$^{-/-}$ mice treated with AAV019-mNrf2 or AAV019-mNrf2^{S335A} at 6 h posts PBS administration. Left panel, Western immunoblots of protein extracts from livers treated with PBS were probed with anti-Flag, or anti-actin. Each lane contains a sample from a single mouse. Right panel, Semi-quantitative result of the blot (n = 3). (B) Serum ALT levels were measured and H&E staining was performed 6 hours after APAP (300 mg/kg) treatment. Scale bars: 10 μm. n = 5 each group, means ± SD. **p <0.01 vs. *Nrf2*$^{-/-}$ mice treated with AAV019-mNrf2 and APAP.

Supplementary Figure 10. Expression of Ho-1 and Gclc in APAP-induced liver injury. WT mice were given APAP (300 mg/kg BW i.p.). (A) Western immunoblots of protein extracts from livers 24 h post APAP were probed with anti-Ho-1, or anti-actin. Each lane contains a sample from a single mouse. (B) Western immunoblots of protein extracts from livers 6 h and 24 h post APAP were probed with anti-Gclc, or anti-actin. Each lane contains a sample from a single mouse. Left panel, Semi-quantitative result of blot. The control (vehicle at the same time point) was set at 1. Values are mean ± SD (n = 3). **p <0.01.

Supplementary Figure 11. Proposed model for the JNK-Nrf2 signaling pathway in mediating liver injury. APAP is metabolized to NAPQI by P450. While NAPQI activates JNK, it also modifies Keap1, leading to the nuclear accumulation of Nrf2. P-JNK phosphorylates the Neh6 domain of Nrf2, leading to increased degradation of the transcription factor. As a result, the Nrf2-directed transcriptional program is inhibited. Dysfunction of the detoxification and cytoprotection system contributes to the liver injury induced by APAP.

Supplementary Table 1. Cloning primers used in the present study.

Plasmid name	Sequence (5’ → 3’)
pET41a-mNrf2^{Neh1}	F: ACGCGGATCCGGTCATCAAAAAGCCCCATTC
	R: CCGCTCGAGCTAAAGATACAAGGTGCTGAGCC
pET41a-mNrf2^{Neh6}	F: ACGCGGATCCGCTTTCAACCCGAAGCACG
	R: CCGCTCGAGCTATGGTGACAGAGGCTGTACTG
pET41a-mNrf2^{Neh3}	F: ACGCGGATCCGAAGTCTTCAGCATGTTACGTG
	R: CCGCTCGAGCTAGTTTTTCTTTGTATCTGGC
pSG5-JNK1	F: TCGAGATGAGCAGAAGCAAGCGTG
	R: GATCCCTGCTGCACCTGTGCTAAAGG
pET41a-JNK1	F: ACAGGATCCATGAGCAGAAGCAAGCGTGAC
	R: ATAGTCGACCTGCTGCACCTGTGCTAAAGG

pETDuet-1-JNK1	F: ACTGGATCCCATGAGCAGAAGCAAGCGTG
	R: ATAGTCGACCTGCTGCACCTGTGCTAAAGG
pETDuet-1-JNK1^{Y185A}	F: GGAACGAGTTTTATGATGACGCCTGCTGTAGTGACTCGCTACTACAGA
	R: TCTGTAGTAGCGAGTCACTACAGCAGGCGTCATCATAAAACTCGTTCC
pETDuet-1-JNK1$^{T183E/Y185E}$	F: GGAACGAGTTTTATGATGGAACCTGAAGTAGTGACTCGCTACTACAGA
	R: TCTGTAGTAGCGAGTCACTACTTCAGGTTCCATCATAAAACTCGTTCC
pcDNA3.1/V5-mNrf2^{S335A}	F: GGAATTCAATGACTCTGACGCTGGCATTTCACTG
	R: CAGTGAAATGCCAGCGTCAGAGTCATTGAATTCC
pETDuet-1-mNrf2$^{\Delta ETGE}$	F: GAAGAGCTCTATGATGGACTTGGAGTTGC
	R: GCCGTCGACCTAGTTTTTCTTTGTATCTG
pETDuet-1-mNrf2$^{\Delta ETGE,S335A}$	F: GAAGAGCTCTATGATGGACTTGGAGTTGC
	R: GCCGTCGACCTAGTTTTTCTTTGTATCTG

pcDNA3.1B/V5-mNrf2$^{\Delta ETGE,335A}$	F: GGAATTCAATGACTCTGACGCTGGCATTTCACTG
	R: CAGTGAAATGCCAGCGTCAGAGTCATTGAATTCC
Fuipw-mNrf2$^{\Delta ETGE}$	F: GACTCTAGAATGGATTACAAGGATGACGATGACAAGATGATGGACTTGGAGTTG CCACCGC
	R: GGAGGCGCGCCTCAGTTTTTCTTTGTATCTGGCTTCTTG
Fuipw-mnrf2$^{\Delta ETGE\Delta SDS1}$	F: GACTCTAGAATGGATTACAAGGATGACGATGACAAGATGATGGACTTGGAGTTG CCACCGC
	R: GGAGGCGCGCCTCAGTTTTTCTTTGTATCTGGCTTCTTG
pEGFP-C1-mNrf2$^{\Delta ETGE\Delta SDS1}$	F: AAGCACGCTGAAGGCACAATGAGTCCCAGCCGAGCGTCCCCAGAGCA
	R: TGCTCTGGGGACGCTCGGCTGGGACTCATTGTGCCTTCAGCGTGCTT
AAV019-mNrf2	F: CTATTTCCGGTGAATTCCTCGAGGCCACCATGATGGACTTGGAGTTGCC

	R: GTTGATTGTTCCAGACGCGTCTATTTGTCGTCATCATCCTTATAGTCCTTA
AAV019-mNrf2^{S335A}	F: CTATTTCCGGTGAATTCCTCGAGGCCACCATGATGGACTTGGAGTTGCC
	R: GTTGATTGTTCCAGACGCGTCTATTTGTCGTCATCATCCTTATAGTCCTTA

Supplementary Table 2 Peptides of His-mNrf2 with modification of phosphorylation detected by mass spectrometric analysis.

Annotated Sequence	**Modifications**	**PhosphoRS: Best Site Probabilities**
HAEGTmEFNDsDSGISLNTSPSR	M6 (Oxidation); S11 (Phospho)	S11 (Phospho): 24.89;
HAEGTmEFNDsDSGISLNTSPSR	M6 (Oxidation); S11 (Phospho)	T5 (Phospho): 24.79

HAEGTmEFNDSDsGISLNTSPSR <u>Ser335</u>	**M6 (Oxidation); S13 (Phospho)**	**S13 (Phospho): 98.47**
HAEGTmEFNDSDsGISLNTSPSR	M6 (Oxidation); S13 (Phospho)	S11 (Phospho): 24.89
ASPEHSVESsIYGDPPPGFSDSEMEELDSAPGSVK	S10 (Phospho)	S9 (Phospho): 49
HAEGTMEFNDsDSGISLNTSPSR	S11 (Phospho)	T5(Phospho): 16.61
HAEGTMEFNDSDsGISLNTSPSR	S13 (Phospho)	T5(Phospho): 16.61
AsPEHSVESSIYGDPPPGFSDSEmEELDSAPGSVK <u>Ser347</u>	**S2 (Phospho); M24 (Oxidation)**	**S10(Phospho): 97.87**
ASPEHSVEsSIYGDPPPGFSDSEMEELDSAPGSVK	S9 (Phospho)	S9(Phospho): 49

HAEGtMEFNDSDSGISLNTSPSR	T5 (Phospho)	T5(Phospho): 16.61
ASPEHSVESSIyGDPPPGFSDSEMEELDSAPGSVK	Y12 (Phospho)	S9(Phospho): 49